Fast warming of the surface ocean under a climatological scenario

Q. Jamet[1*], W. K. Dewar[1], N. Wienders[1] and B. Deremble[2]

[1]Department of Earth, Ocean and Atmospheric Science, the Florida State University, Tallahassee, Florida
[2]Laboratoire de Météorologie Dynamique, Paris, France

Key Points:

- Weakly varying climatological winds reduce upper ocean vertical mixing, affecting the redistribution of surface radiative forcing
- Coupled to an atmospheric boundary layer, the modeled ocean response to climatological winds is to warm up considerably at the surface
- Results illustrate the pivotal improvements in air-sea interactions achieved by driving an ocean model with an atmospheric boundary layer

*The Florida State University, 117 N Woodward Avenue, Tallahassee, FL 32306-4320.

Corresponding author: Quentin Jamet, `qjamet@fsu.edu`

Abstract

We examine various strategies for forcing ocean-only models, focusing primarily on an atmospheric boundary layer model. This surface forcing allows air-sea exchanges to affect atmospheric temperature and relative humidity, relaxing the assumption of an artificially large atmospheric heat capacity made if these variables are prescribed. When exposed to climatological winds, the simulated North Atlantic oceanic temperature warms considerably at the surface as compared to a model with full atmospheric variability. This warming is mainly explained by a weakened upper ocean vertical mixing in response to the weakly varying climatological winds. Specifying the atmospheric temperatures inhibits this warming, but depends on the unrealistic large atmospheric heat capacity. We thus interpret the simulated warmer ocean as a more physically consistent ocean response. We conclude the use of an atmospheric boundary layer model provides many benefits for ocean only modeling, although strategies for maintaining high frequency winds in climatologies are require.

1 Introduction

Understanding the origin of the low frequency oceanic variability is an open subject of research. While it is recognized that the atmosphere drives the ocean circulation on short time scales, its contribution at longer time scales remains debated (Clement et al., 2015; Farneti et al., 2017; Zhang et al., 2016). Studies have attempted to disentangle the respective role of the ocean and the atmosphere in climate variability from observations (McCarthy et al., 2015), but most assess this question with the use of ocean models. A common numerical approach is to compare the oceanic response to a prescribed atmosphere simulated by twin numerical experiments (e.g. Penduff et al., 2011; Sérazin et al., 2015), one driven by a realistic atmosphere, the other by a climatological atmosphere. We study ocean-only models forced by different surface forcing strategies with the view toward assessing strengths and weaknesses of each. In this study we focus on the behaviour of the oceanic temperature, salinity is under study.

Modeling a variable ocean under a specified but variable atmosphere is a useful and efficient idealization. However, Huck and Vallis (2001) have highlighted an important caveat of this approach for the growth of large scale modes of variability in idealized ocean models (Colin de Verdière et al., 1999; Huck et al., 1999). They found that these modes of variability only appear if the ocean model was forced by prescribed fluxes rather than a prescribed atmosphere. In the first case (prescribed air-sea fluxes), the ocean is not as constrained as in the second case where the atmospheric conditions maintain the ocean in a state close to the forcing conditions. Their results illustrate the limitations associated with a prescribed atmospheric forcing, where the assumption of an infinite heat capacity for the atmosphere inhibits the development of internal ocean dynamics.

Following Huck and Vallis (2001), we wish to assess if similar limitations would be at work for the development of an oceanic state under climatological winds. This question arises from the recognized impacts of the fast varying atmospheric winds on both turbulent air-sea fluxes and upper ocean vertical mixing. Several studies have revealed that the high frequency atmospheric dynamics control a significant portion of both turbulent air-sea fluxes (Gulev, 1994; Hughes et al., 2012; Jung et al., 2014; Ponte & Rosen, 2004; Wu et al., 2016; Zhai et al., 2012) and vertical mixing in the upper ocean (Condron & Renfrew, 2013; Holdsworth & Myers, 2015; Wu et al., 2016). Fig. 1 (top panels) compares the high frequency standard deviation of the wind speed $|u| = \sqrt{u^2 + v^2}$ in the North Atlantic between the fully varying winds and the climatological winds. At high latitudes, where the atmospheric dynamics are mostly controlled by transient features like synoptic weather systems, the high frequency standard deviation is 2 to 3 times stronger in the fully varying product. Then, forcing an ocean model with climatological winds is expected to significantly modify air-sea fluxes and upper ocean vertical mixing, which ultimately leads to an ocean state that is significantly different from the realistic ocean state.

By prescribing the state of the atmosphere, the ocean surface temperature is constrained to remain near the atmospheric temperature. To identify the ocean state that develops under climatological winds, we propose to work with an atmospheric boundary layer for which the atmospheric temperature and humidity are prognostic variables (CheapAML; Deremble et al., 2013). With such a boundary layer, we relax the assumption that the atmosphere is a fluid with an infinite heat capacity and allow it to respond to ocean surface structures. We then quantify the impact of climatological winds on the simulated oceanic state by comparing the time evolution of a pair of ocean simulation, one driven by the fully varying winds and the other by climatological winds. A detailed description of the model strategy is given in Section 2. The main differences between the pair experiments using CheapAML are described in Section 3, and we compare these results with those obtained with a more traditional representation of air-sea fluxes, i.e. when the atmosphere is prescribed, in Section 4. Finally, we conclude and discuss the results in Section 5.

2 Numerical Experiments

We use the MIT general circulation model (MITgcm; Marshall et al., 1997) in a regional configuration of the North Atlantic: the domain extends from 20°S to 55°N with a horizontal resolution of $\frac{1}{4}^{\circ}$ (see Supporting Information for additional details). We use the non-local K-Profile Parametrization (KPP) scheme of Large et al. (1994) with a critical Richardson number of 0.3 to parametrize the vertical mixing in the upper ocean boundary layer. The mixed layer depth (MLD) computed by this parameterization will be used in the heat budget of Section 3.2.

At the surface, different strategies are used to force the ocean model and look at their impact on the ocean dynamics. In a first set of experiments, we couple the ocean model to the atmospheric boundary layer model CheapAML (Deremble et al., 2013). With this approach, we better represent the air-sea exchanges, and we also let the ocean develop its internal dynamics (not necessarily correlated to a prescribed atmospheric state). In CheapAML, winds are assumed to be the least sensitive atmospheric variable to ocean surface structure. The remaining atmospheric variables, i.e. temperature and humidity, are then advected by these winds and are modified by the air sea fluxes. Over the ocean, the temporal evolution of these atmospheric variables is computed using an advection-diffusion equation (see Supporting Information and Deremble et al., 2013). Over land, temperature and humidity are strongly relaxed toward the reanalysis prescribed values. The components of the net heat fluxes at the bottom of the boundary layer model (Q_{net}, positive upward) that influence these atmospheric variables are: (i) prescribed downward shortwave radiation, (ii) longwave radiation (the sum of prescribed downward longwave radiations and outgoing longwave radiations), and (iii) latent and sensible heat fluxes, computed with the bulk formula of the Coupled Ocean-Atmosphere Response Experiment, version 3 (COARE3, Fairall et al., 2003). The atmospheric variables prescribed in CheapAML, i.e. solar shortwave and downward longwave radiation, precipitation, atmospheric temperature and relative humidity over land and zonal and meridional wind components, are applied every 6 hours and derived from the Drakkar forcing set (cf Supporting Information).

This configuration is run for 10 years in two different experiments. In the first one, we use the full range of atmospheric time scales, from sub-daily (6-hourly) to interannual, over the period 1958-1967 for the wind and atmospheric thermodynamic variables on land. In the second one, we use a yearly repeated climatological atmospheric seasonal cycle. To consistently filter the year-to-year atmospheric variability, the climatology has been computed as an ensemble average of all the years between 1958-1977. We name these two experiments AML_FULL and AML_CLIM respectively.

To understand how the atmospheric temperature and humidity in CheapAML respond to the ocean surface dynamics, two additional experiments are conducted where all atmospheric variables (wind, temperature and humidity) are prescribed. This strategy is commonly used in the ocean modeling community and it will serve as a reference test case to which we will compare our experiments. With these prescribed atmospheric variables, we compute the air-sea fluxes the same way as the previous cases but there is no feedback on the atmospheric temperature and humidity. As in AML_FULL and AML_CLIM we run two experiments with either fully varying or climatological winds, and are referred to as FORC_FULL and FORC_CLIM, respectively. We compare these experiments in Section 4.

3 Fully Varying vs Climatological Wind Experiments

Because the Sea Surface Temperature (SST) is an oceanic variable sensitive to air-sea exchange, we first compare the simulated SST for the two experiments AML_CLIM and AML_FULL (Fig. 2, top panels) after 10 years of simulation. The yearly averaged SST differences between the two experiments are very large in amplitude, reaching more than 8°C in the subtropical gyre, and spreading over the North Atlantic, north of 20°N. At the center of the subtropical gyre where the largest SST differences are observed, the time evolution of SST over the course of the 10 years of simulation reveals that such large differences are reached quickly, after 5 months, suggesting a fast dynamic response of the ocean. The mechanism that drives the warming of the subtropical gyre in the AML_CLIM experiment is described in the two following sections.

3.1 Heat Fluxes

In our configuration, the components of the net heat fluxes which vary from experiment to experiment are the latent and sensible fluxes, as well as the outgoing longwave radiation associated with the SST (the other components are prescribed). We discuss their respective contribution for the net heat fluxes in the following.

In the experiment with fully varying winds, the time mean and standard deviation of the latent and sensible heat fluxes (computed over the 10 years of simulation) are 117±37 and 8±8 $\mathrm{W\,m^{-2}}$, respectively. Added together, these fluxes are sufficiently strong to induce positive (upward) net heat fluxes during the first two months of simulation (Fig. 3, top panel). They contribute to the cooling of the ocean surface at the beginning of the simulation which is consistent with winter time (January-February). In the experiment with climatological winds, the turbulent fluxes are reduced by more than 50% (57±19 W $\mathrm{m^{-2}}$; 1±1.4 W $\mathrm{m^{-2}}$ for latent and sensible heat fluxes, respectively), consistent with earlier results (Hughes et al., 2012). As a consequence, the too weak latent plus sensible heat fluxes lead to negative (downward) net heat fluxes, contributing to the warming of the surface ocean at the beginning of the simulation (top right panel of Fig. 2).

The mechanisms that drive this reduction of turbulent air-sea fluxes are further investigated by looking at the sensible heat flux amplitude $S = C_d|\mathbf{u}|(SST - T_a)$ as a function of the two main contributing factors, i.e. the wind speed $|\mathbf{u}|$ and the air-sea temperature difference $(SST{-}T_a)$ (right panels of Fig. 3). As a response to a weaker wind variance in AML_CLIM, there are no wind stronger than 5 m $\mathrm{s^{-1}}$ (top right panel). However, for wind speed weaker than 5 m $\mathrm{s^{-1}}$, the sensible heat fluxes in AML_CLIM remain weaker than those obtained under fully varying winds, suggesting that the changes in air-sea fluxes are not only driven by the weaker climatological wind speed $|\mathbf{u}|$. The other parameter that contributes to the strength of the sensible heat fluxes is the air-sea temperature difference $SST - T_a$. In AML_CLIM, the air-sea temperature differences do not exceed ±1°C (Fig. 3, bottom right panel), while they range from about -2°C to about +4°C in AML_FULL. Under fully varying winds, there are thus oceanic processes that take the ocean surface away from the overlying atmosphere and lead to larger air-sea temperature differences. We show in Section 3.2 that those processes are associated with upper ocean vertical mixing.

As the ocean surface quickly warms up at the beginning of the simulation when exposed to climatological winds, the outgoing longwave radiation increases accordingly (outgoing longwave radiation is proportional to SST^4). The system reaches a new state after 5 months with a new SST about 8°C warmer than for the fully varying wind experiment. Note that the upward longwave radiation is 40-50 W m^{-2} stronger in the climatological wind experiment. This balances about 80% of the -60 W m^{-2} time mean difference in turbulent heat fluxes, thus preventing the SST difference to be greater than 8°C. After the 5 months of initial transition, the model slowly drifts toward its new state of equilibrium with an SST trend in the subtropical gyre that is about +0.15°C/yr larger than the experiment driven by fully varying winds.

3.2 Oceanic Vertical Mixing

We now describe the differences between the two equilibria in terms of oceanic dynamics. For this purpose, we performed a heat budget following Peter et al. (2006) for the box at the center of the subtropical gyre where the SST difference is the largest. The temperature tendency $\partial_t \langle T \rangle$ within the mixed layer $h(x, y, t)$ (computed by the KPP parameterization) is decomposed into advective terms, a flux term and dissipation terms (cf Supporting Information for more details). Comparing the results of this heat budget for the two experiments using CheapAML (Fig. 4), the most important difference in the processes controlling the temperature is found to be the upper ocean vertical mixing.

During winter, the atmospheric storms that contribute to high frequency wind speed variance in AML_FULL induce a mixing in the upper 40-50 m, redistributing the surface heat fluxes downward, leading to a weak temperature tendency (Fig. 4, top panel). During summer, the depth of the mixed layer reduces to about 10 m due to the weaker wind variance and the surface heat fluxes increase. The temperature tendency induced by the surface heating $-\frac{Q_{net}}{\rho_0 C_p h}$ thus increased to about 0.5 °C/day, but is balanced by dissipative and advective processes, such that the total temperature tendency within the mixed layer does not exceed 0.1 °C/day. The vertical diffusion at the bottom of the mixed layer $\frac{1}{h} K_z \partial_z T|_{z=-h}$ controls most of this balance. It explains a significant fraction of the residual between the total temperature tendency and the action of surface heating $resid. = \partial_t \langle T \rangle + \frac{Q_{net}}{\rho_0 C_p h}$, while the advective terms, the horizontal dissipative term and the entrainment term are at least one order of magnitude smaller.

In AML_CLIM by contrast (Fig. 4, bottom panel), the depth of the mixed layer is much smaller and relatively constant through the year, with values that do not exceed 15 m during winter. As a consequence, the temperature tendency induced by air-sea fluxes exceeds 0.5 °C/day most of the time. In this experiment however, the diffusive fluxes at the bottom of the mixed layer explain only a small fraction of the residual. This result suggests that the oceanic processes that balance the excess of heat induced by the surface heating have changed. We suspect night time convection comes into play, but we cannot draw firm conclusions with the 5-day averaged outputs used in this study.

The large reduction in mixed layer depth is observed all over the domain, where the maximum depth of the mixed layer computed by the KPP parameterization is about 3 to 4 times shallower North of 20°N in AML_CLIM (Fig. 1, bottom panels). This spatial pattern resembles the wind variance (top panels). In fact, in AML_FULL, the high frequency wind variance induces a vertical velocity shear $\partial_z \mathbf{u}$ in the upper layers, that destabilizes the ocean: the Richardson number $R_i = \frac{N^2}{\partial_z \mathbf{u}}$ (with N^2 the buoyancy frequency) decreases, and ultimately falls below a critical value ($R_i = 0.3$ in our configuration). For such a low Richardson number, the vertical structure of the ocean is unstable to shear instability, and vertical mixing occurs. In AML_CLIM by contrast, the vertical velocity shear is much weaker in response to the weaker high frequency variance of the climatological winds, and the ocean is more stable. If less mixing occurs in the upper ocean, the surface heat fluxes induce a fast warming of the upper ocean.

4 A Prescribed Atmosphere

Most numerical studies that use climatological atmospheric fields do not use an atmosphere boundary layer model to compute the atmospheric temperature and humidity (Grégorio et al., 2015; Penduff et al., 2011; Sérazin et al., 2015). In order to compare our results with these kind of experiments, we perform two additional runs (FORC_FULL and FORC_CLIM) for which all atmospheric fields (including temperature and humidity) are prescribed. After 10 years of simulation, the SST difference between FORC_FULL and FORC_CLIM share a relatively similar spatial pattern with the AML experiments (Fig. 2, left panels), but those differences are much weaker, and do not exceed 2.5°C in the subtropical gyre. Note that, consistent with the temperature difference observed between the two AML experiments, the SST difference observed in the subtropical gyre is also reached after only 5 months of simulation (Fig. 2, right panels).

From these comparisons, we conclude that prescribing the atmospheric state reduces the effects of climatological winds on the temperature of the upper ocean layers. The underlying physical basis remains however questionable. Due to the weak high frequency variance of the climatological winds, the vertical ocean mixing remains weak. The difference in the mixed layer depth computed by the KPP scheme is very similar to what is shown in Fig. 1 for the AML experiments. As a consequence, the upper ocean tends to warm up in FORC_CLIM, but the atmosphere does not. In fact, because the atmospheric temperature is prescribed in this experiment, the ocean-atmosphere temperature differences increase, as shown in Fig. 3 (bottom right panel) for the subtropical gyre. In the FORC_CLIM experiment, the $SST - T_a$ difference is always positive and roughly 2-4°C. This illustrates the damping role of the atmosphere on the surface ocean temperatures, constraining the upper ocean warming tendency. This increased $SST - T_a$ difference counteracts the effect of climatological winds on the turbulent air-sea fluxes, such that for the same wind speed amplitude, the sensible heat fluxes are much larger in FORC_CLIM than in AML_CLIM and always positive (Fig. 3, top right panel). A similar scenario happens for the latent heat fluxes, which results in turbulent heat fluxes in the FORC_CLIM experiment which are of comparable amplitude those found in the FORC_FULL experiment (Fig. 3, bottom panel). This is not consistent with previous studies (Gulev, 1994, 1997; Hughes et al., 2012), where the lack of high frequency wind variance is expected to significantly reduce the magnitude of turbulent air-sea fluxes. In the AML experiments by contrast, since the atmospheric temperature follows the surface ocean warming we have shown that the reduced turbulent heat fluxes under climatological winds are consistently captured and balanced by increased outgoing longwave radiations. Since this latter scenario has better physical consistency, we argue that, when exposed to an artificial climatological atmosphere, the ocean response is to warm up considerably at the surface.

5 Conclusion

We have revisited in this study the model strategy used to represent air-sea interactions in ocean-only models. The analysis of an ocean model in a regional North Atlantic configuration coupled to an atmospheric boundary layer model shows that the use of climatological winds leads to a fast warming of the upper ocean layers, reaching up to 8 °C in the North Atlantic subtropical gyre after only 5 months of simulation. Although the oceanic state at the end of the simulation differs from the oceanic state in a companion experiment driven by fully varying winds, we argue that those changes are physically consistent, and interpret the simulated oceanic state as likely when exposed to an artificial climatological atmosphere. A side effect of climatological averaging is to act as a low-pass filter, and the resulting wind product does not contain fast varying synoptic weather systems. Those high frequency wind events play a significant role for both turbulent air-sea fluxes and upper ocean vertical mixing.

In the climatological scenario, the system reaches a new balance for which the warmer ocean surface induced by weak ocean vertical mixing is balanced by increased outgoing longwave radiation. This balance is quite different from the equilibrium reached in the traditional approach (where the atmospheric state is prescribed). In the latter case, the ocean vertical mixing remains weak, but the effects of the climatological winds on the turbulent air-sea fluxes are balanced by an increased contribution of the difference between the warming ocean and the prescribed atmosphere. The turbulent air-sea fluxes are strengthened and the atmosphere controls the surface ocean dynamics by damping the surface warming tendency. However, this 'traditional' approach relies on the unrealistic assumption of an infinite heat capacity for the atmosphere, whereas the ocean is more appropriately approximated as the slow climate component since its heat capacity is much larger than that of the atmosphere. Those results suggest that the use of an atmospheric boundary layer model rather than a prescribed atmosphere when decoupling an ocean model from the atmosphere is a more suitable strategy to better represent the physics of the air-sea turbulent fluxes. Finally, improvements in the salinity have been seen under the CheapAML scenario. This will be the subject of a further contribution.

To isolate the oceanic dynamics from the low frequency atmospheric forcing when an ocean model is coupled to an atmospheric boundary layer model, one thus needs a wind product that does not contain any interannual and longer variability but which accounts for the fast varying winds. A 'normal' year strategy similar to that proposed by Large and Yeager (2004) to force the Coordinated Ocean-ice Reference Experiments (COREs, Griffies et al., 2009), which consists of using the atmospheric state of a given year and to repeat this forcing every year, is an attractive approach to conduct such sensitivity experiments. Note however that high frequency white noise atmospheric forcing might also induce a low frequency oceanic variability (Frankignoul & Hasselmann, 1977; Frankignoul et al., 1997).

Acknowledgments

We thank Camille Lique for a constructive discussion and references. We thank Bernard Barnier and its collaborators for providing us the Drakkar Forcing Sets data and the expertise for using them. This work was supported by NSF Grant OCE-1537304.

References

Clement, A., Bellomo, K., Murphy, L. N., Cane, M. A., Mauritsen, T., Rädel, G., & Stevens, B. (2015). The atlantic multidecadal oscillation without a role for ocean circulation. *Science*, *350*(6258), 320–324.

Colin de Verdière, A., & Huck, T. (1999). Baroclinic instability: An oceanic wavemaker for interdecadal variability. *J. Phys. Oceanogr.*, *29*(5), 893–910.

Condron, A., & Renfrew, I. A. (2013). The impact of polar mesoscale storms on northeast Atlantic Ocean circulation. *Nature Geoscience*, *6*(1), 34.

Deremble, B., Wienders, N., & Dewar, W. (2013). Cheapaml: A simple, atmospheric boundary layer model for use in ocean-only model calculations. *Mon. Wea. Rev.*, *141*(2), 809–821.

Fairall, C., Bradley, E. F., Hare, J., Grachev, A., & Edson, J. (2003). Bulk parameterization of air–sea fluxes: Updates and verification for the coare algorithm. *J. Clim.*, *16*(4), 571–591.

Farneti, R. (2017). Modelling interdecadal climate variability and the role of the ocean. *Wiley Interdisciplinary Reviews: Climate Change*, *8*(1).

Frankignoul, C., & Hasselmann, K. (1977). Stochastic climate models, part ii application to sea-surface temperature anomalies and thermocline variability. *Tellus*, *29*(4), 289–305.

Frankignoul, C., Müller, P., & Zorita, E. (1997). A Simple Model of the Decadal Response of the Ocean to Stochastic Wind Forcing*. *J. Phys. Oceanogr.*, *27*(8), 1533–1546.

Grégorio, S., Penduff, T., Sérazin, G., Molines, J.-M., Barnier, B., & Hirschi, J. (2015). Intrinsic variability of the atlantic meridional overturning circulation at interannual-to-multidecadal time scales. *Journal of Physical Oceanography*, *45*(7), 1929–1946.

Griffies, S. M., Biastoch, A., Böning, C., Bryan, F., Danabasoglu, G., Chassignet, E. P., ... others (2009). Coordinated ocean-ice reference experiments (cores).

Ocean Model., *26*(1-2), 1–46.

Gulev, S. K. (1994). Influence of space-time averaging on the ocean-atmosphere exchange estimates in the north atlantic midlatitudes. *J. Phys. Oceanogr.*, *24*(6), 1236–1255.

Gulev, S. K. (1997). Climatologically significant effects of space–time averaging in the north atlantic sea–air heat flux fields. *Journal of climate*, *10*(11), 2743–2763.

Holdsworth, A. M., & Myers, P. G. (2015). The influence of high-frequency atmospheric forcing on the circulation and deep convection of the Labrador Sea. *J. Clim.*, *28*(12), 4980–4996.

Huck, T., Colin de Verdière, A., & Weaver, A. J. (1999). Interdecadal variability of the thermohaline circulation in box-ocean models forced by fixed surface fluxes. *J. Phys. Oceanogr.*, *29*(5), 865–892.

Huck, T., & Vallis, G. K. (2001). Linear stability analysis of three-dimensional thermally-driven ocean circulation: application to interdecadal oscillations. *Tellus*, *53A*, 526–545.

Hughes, P. J., Bourassa, M. A., Rolph, J. J., & Smith, S. R. (2012). Averaging-related biases in monthly latent heat fluxes. *J. Atmos. Ocean. Technol.*, *29*(7), 974–986.

Jung, T., Serrar, S., & Wang, Q. (2014). The oceanic response to mesoscale atmospheric forcing. *Geophys. Res. Lett.*, *41*(4), 1255–1260.

Large, W. G., McWilliams, J. C., & Doney, S. C. (1994). Oceanic vertical mixing: A review and a model with a nonlocal boundary layer parameterization. *Rev. Geophys.*, *32*(4), 363–403.

Large, W. G., & Yeager, S. G. (2004). Diurnal to decadal global forcing for ocean and sea-ice models: the data sets and flux climatologies.

Marshall, J., Adcroft, A., Hill, C., Perelman, L., & Heisey, C. (1997). A finite-volume, incompressible Navier Stokes model for studies of the ocean on parallel computers. *J. Geophys. Res.*, *102*(C3), 5753–5766.

McCarthy, G. D., Haigh, I. D., Hirschi, J. J.-M., Grist, J. P., & Smeed, D. A. (2015). Ocean impact on decadal Atlantic climate variability revealed by sea-level observations. *Nature*, *521*(7553), 508–510.

Penduff, T., Juza, M., Barnier, B., Zika, J., Dewar, W. K., Treguier, A.-M., … Audiffren, N. (2011). Sea level expression of intrinsic and forced ocean variabilities at interannual time scales. *J. Clim.*, *24*(21), 5652–5670.

Peter, A.-C., Le Hénaff, M., Du Penhoat, Y., Menkès, C. E., Marin, F., Vialard, J., … Lazar, A. (2006). A model study of the seasonal mixed layer heat budget in the equatorial Atlantic. *Journal of Geophysical Research: Oceans*, *111*(C6).

Ponte, R. M., & Rosen, R. D. (2004). Nonlinear effects of variable winds on ocean stress climatologies. *J. Clim.*, *17*(6), 1283–1293.

Sérazin, G., Penduff, T., Grégorio, S., Barnier, B., Molines, J.-M., & Terray, L. (2015). Intrinsic variability of sea level from global ocean simulations: Spatiotemporal scales. *J. Clim.*, *28*(10), 4279–4292.

Wu, Y., Zhai, X., & Wang, Z. (2016). Impact of synoptic atmospheric forcing on the mean ocean circulation. *J. Clim.*, *29*(16), 5709–5724.

Zhai, X., Johnson, H. L., Marshall, D. P., & Wunsch, C. (2012). On the wind power input to the ocean general circulation. *J. Phys. Oceanogr.*, *42*(8), 1357–1365.

Zhang, R., Sutton, R., Danabasoglu, G., Delworth, T. L., Kim, W. M., Robson, J., & Yeager, S. G. (2016). Comment on the atlantic multidecadal oscillation without a role for ocean circulation. *Science*, *352*(6293), 1527–1527.

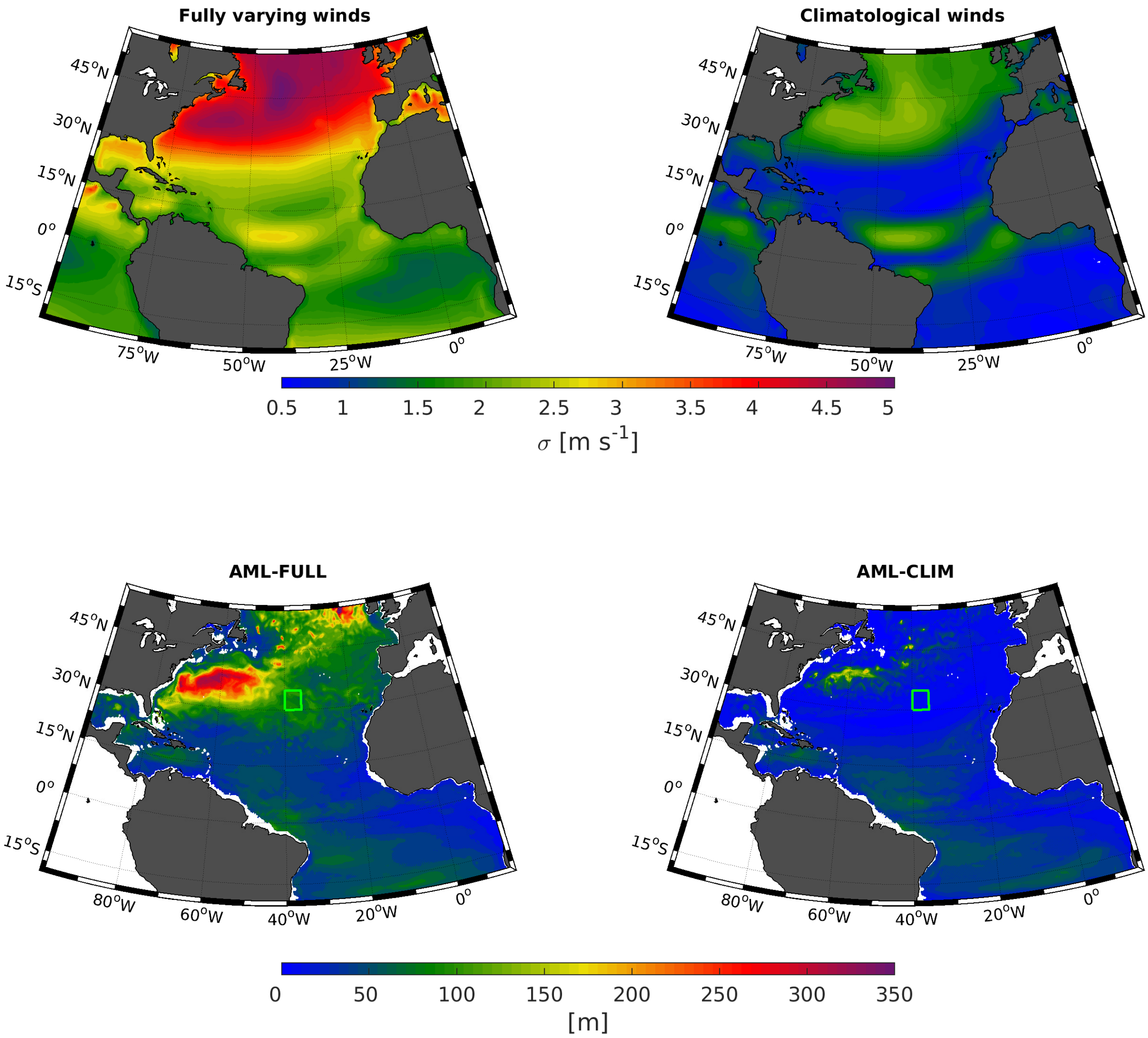

Figure 1. (Top) Seasonal standard deviation σ [m s^{-1}] of the wind speed $||u|| = \sqrt{u^2 + v^2}$ for the fully varying (left) and the climatological (right) winds. Data are from the Drakkar Forcing Set, version 4.4. The climatology has been computed over the period 1958-1977, and the seasonal standard deviation of the fully varying winds has been averaged over this period. (Bottom) Maximum depth of the mixed layer [m] computed by the KPP parameterization during the first year of simulation for the AML_FULL (left) and the AML_CLIM (right) experiments.

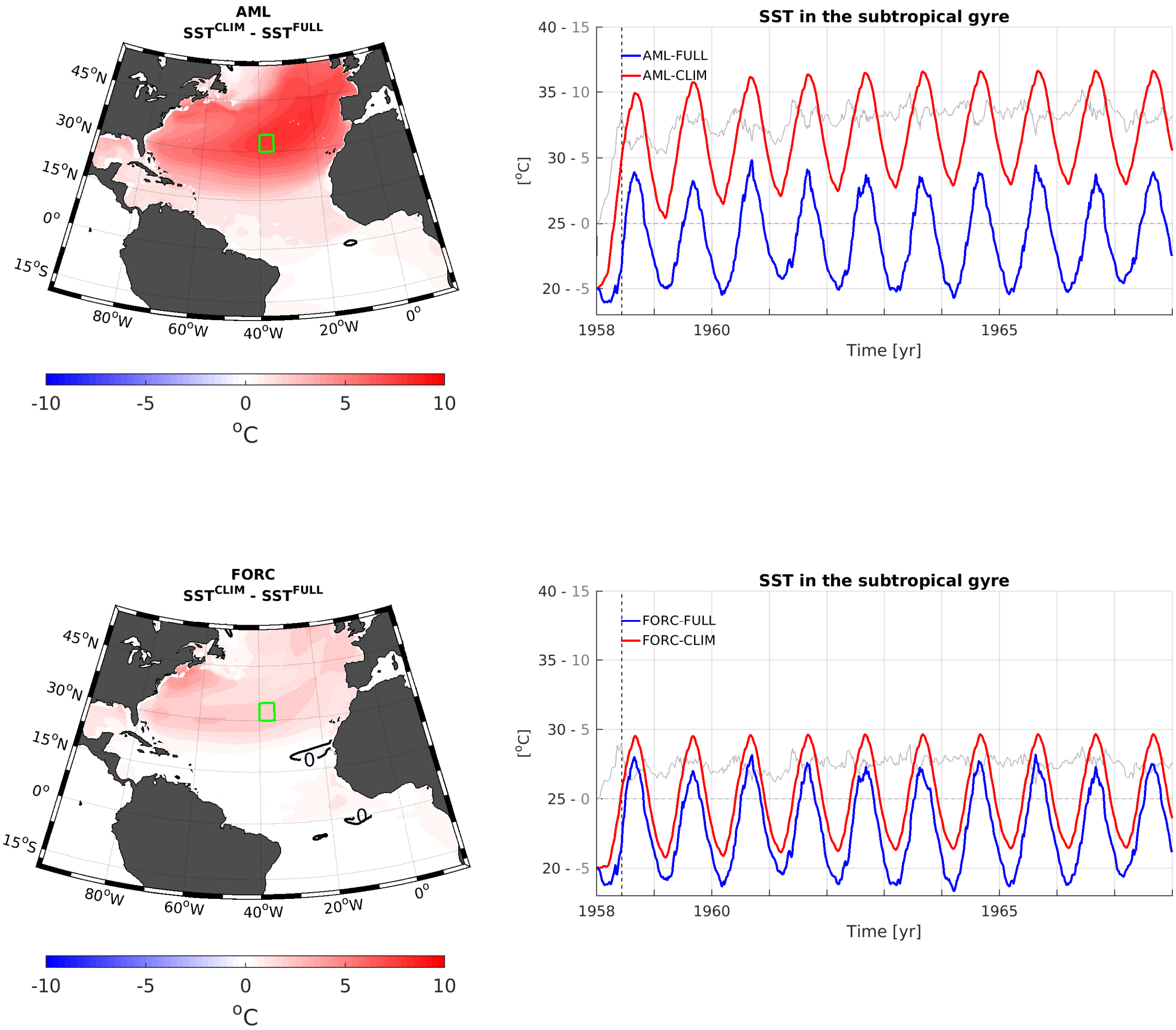

Figure 2. (Top) Yearly averaged SST difference between the AML_CLIM and the AML_FULL experiment for the last year of simulation (left), and (right) spatially averaged SST in the subtropical gyre ([40-35W;30-35N], green box on the left panel) for the AML_CLIM (red line) and the AML_FULL (blue line) experiments. The gray line is the difference between the two, with the associated scale on the left in gray. (Bottom) Same as top panels, but for the FORC experiments discussed in Section 4.

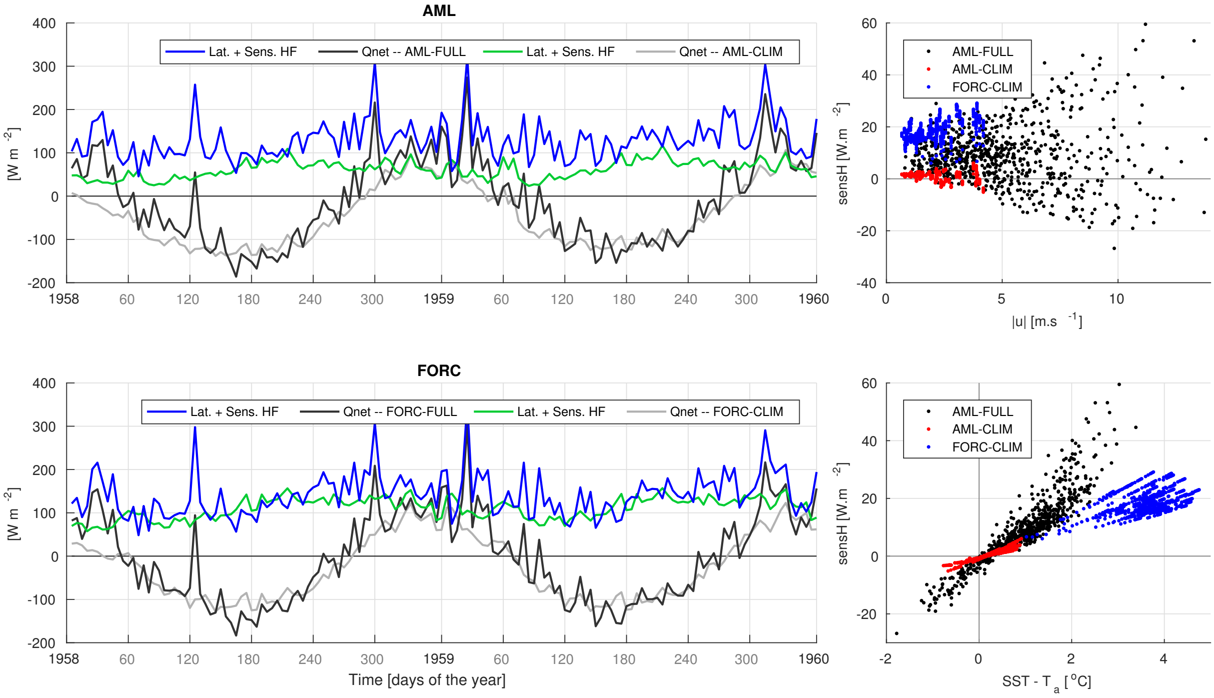

Figure 3. (Top left) Spatially averaged net heat fluxes Q_{net} (positive upward, [W m^{-2}]) at the center of the subtropical gyre (green box of Fig. 2, left panels) for the AML_FULL (drak gray line) and the AML_CLIM (light gray line) experiments, and the associated contribution of the latent plus sensible heat fluxes (blue and green lines, respectively). (Bottom left) Same as top left panel but for the FORC_FULL and the FORC_CLIM experiments. (Right) Scatter plots of the sensible heat fluxes as a function of the wind speed (top) and the air-sea temperature difference SST-T_a (bottom) for the experiment AML_FULL (black), AML_CLIM (red) and FORC_CLIM (blue). The data correspond to the spatial average within the green box of Fig. 2, left panels, and for the 10 years long time series.

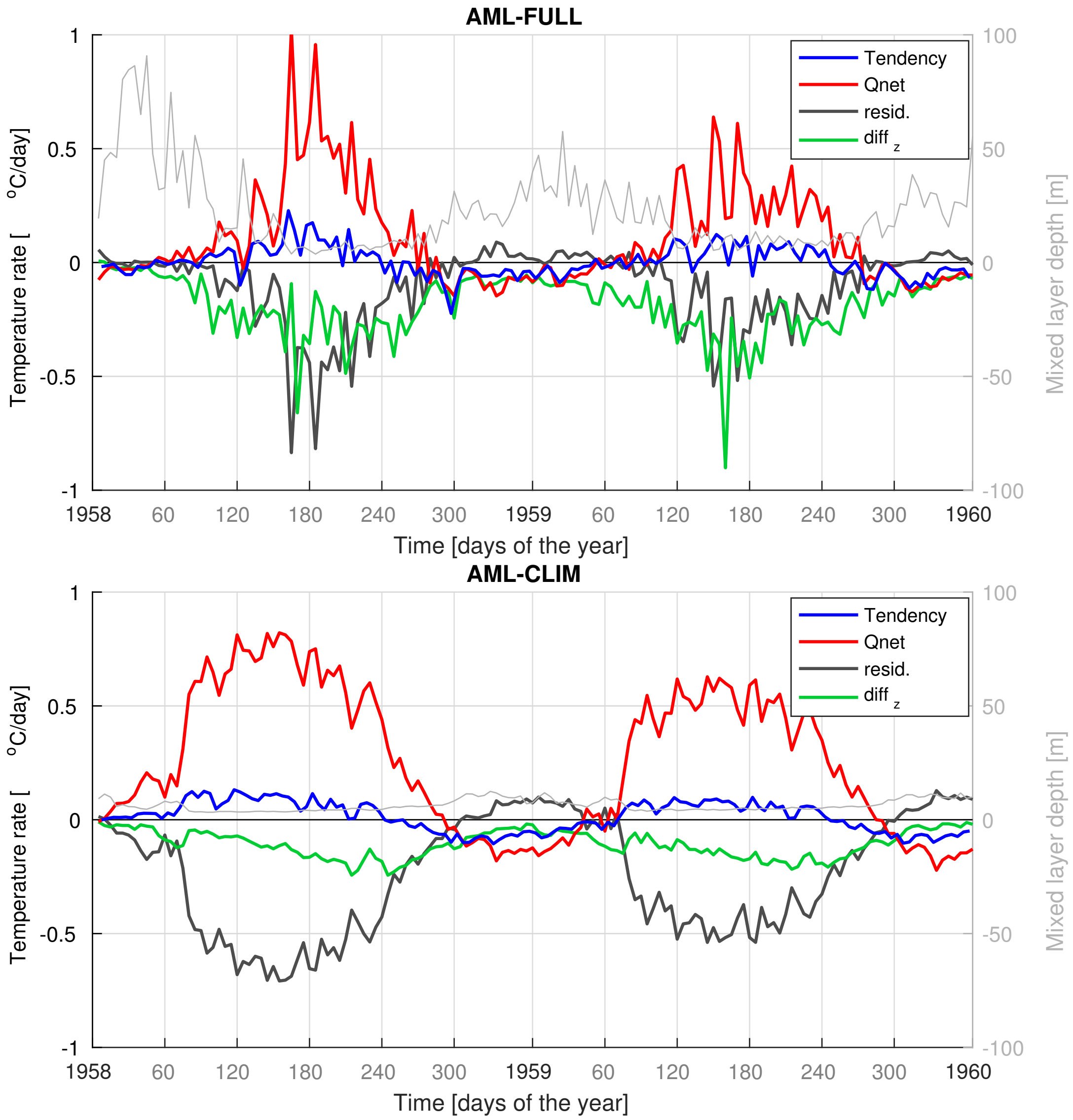

Figure 4. Contribution of the net heat fluxes $-\frac{Q_{net}}{\rho_0 C_p h}$ (red line, Q_{net} positive upward) and the vertical diffusion at the bottom of the mixed layer $\frac{1}{h}K_z\partial_z T|_{z=-h}$ (green line) for the temperature tendency $\partial_t \langle T \rangle$ (blue line) within the mixed layer (see Supporting Informations) for the AML_FULL (top) and the AML_CLIM (bottom) experiments. The total contribution of dissipative terms is computed as a residual $resid. = \partial_t \langle T \rangle + \frac{Q_{net}}{\rho_0 C_p h}$, and is shown in dark gray. The light thine gray line represents the depth of the mixed layer, with the associated axe on the right. The budget is made at the center of the subtropical gyre (green box of Fig. 2, left panels).